Two novel phospholipid hydroperoxide glutathione peroxidase genes of *Paragonimus westermani* induced by oxidative stress

S.-H. KIM[1,3]†, G.-B. CAI[1,§†], Y.-A. BAE[1,3], E.-G. LEE[1,3], Y.-S. LEE[2,3] *and* Y. KONG[1,3]*

[1] *Department of Molecular Parasitology, Sungkyunkwan University School of Medicine, Suwon, 440-746, Korea*
[2] *Department of Pharmacology, Sungkyunkwan University School of Medicine, Suwon, 440-746, Korea*
[3] *Center for Molecular Medicine, Samsung Biomedical Research Institute, Suwon, 440-746, Korea*

(*Received 1 December 2008; revised 6 January 2009; accepted 12 January 2009; first published online 6 March 2009*)

SUMMARY

Phospholipid hydroperoxide glutathione peroxidase (PHGPx; GPx4) plays unique roles in the protection of cells against oxidative stress by catalysing reduction of lipid hydroperoxides. We characterized 2 novel *GPx* genes from a lung fluke, *Paragonimus westermani* (designated *PwGPx1* and *PwGPx2*). These single copy genes spanned 6559 and 12 371 bp, respectively, and contained each of 5 intervening introns. The *PwGPx2* harboured a codon for Sec and a Sec insertion sequence motif. Proteins encoded by the *Paragonimus* genes demonstrated a primary structure characteristic to the PHGPx family, including preservation of catalytic and glutathione-binding domains and absence of the subunit interaction domain. Expression of *PwGPx1* increased gradually as the parasite matured, whereas that of *PwGPx2* was temporally regulated. *PwGPx2* was expressed at the basal level from the metacercariae to the 3-week-old juveniles; however, the expression was significantly induced in the 7-week-old immature worms and reached a plateau in the 12-week-old adults and eggs. PwGPx1 and PwGPx2 were largely localized in vitellocytes within vitelline glands and eggs. Oxidative stress-inducible paraquat, juglone and H_2O_2 substantially augmented the *PwGPx1* and *PwGPx2* expressions in viable worms by 1·5- to 11-fold. Our results strongly suggested that PwGPxs may actively participate in detoxification of oxidative hazards in *P. westermani*.

Key words: *Paragonimus westermani*, antioxidants, phospholipid hydroperoxide glutathione peroxidase, vitellocytes, oxidative stress.

INTRODUCTION

Reactive oxygen species (ROS) are inevitably generated through incomplete respiration in mitochondria, as by-products of a variety of metabolic reactions or by exogenous stimuli including irradiation and redox-cycling drugs (Tawe *et al*. 1998; Chi *et al*. 2005). ROS play pivotal roles not only in control of cellular redox homeostasis (Jackson, 2005) but also in induction of cellular proliferation or apoptosis by activating signaling molecules (Thannickal and Fanburg, 2000; Hancok *et al*. 2001; Sim *et al*. 2005). However, the unbalanced generation of ROS exerts harmful effects. It might induce breakage of DNA strands, protein oxidation, polysaccharide depolymerization, membrane-lipid peroxidation and impairment of signal transduction from membrane receptors in various physiological processes (Dröge, 2002). The aerobic organisms have evolved a series of multi-layered enzymatic and non-enzymatic defence systems, which can remove the aggressive ROS and/or repair ROS-mediated cell damage.

Glutathione peroxidase (GPx; EC 1.11.1.9) encompasses 6 distinct families of multiple isoenzymes, which catalyse the reduction of H_2O_2, organic hydroperoxides and lipid hydroperoxides by using glutathione as a reducing agent. The GPx families share similar structural and enzymatic properties with one another, and these selenium-dependent enzymes act as a tetramer via the mediation of a subunit interaction domain (Arthur, 2000). In contrast, GPx proteins categorized into GPx4 family (phospholipid hydroperoxide GPx, PHGPx; E.C. 1.11.1.12) have a series of distinct features compared to the other GPx families. PHGPxs function in a monomeric form because they lack the subunit interaction domain (Epp *et al*. 1983; Brigelius-Flohé *et al*. 1994; Arthur, 2000). These molecules exhibit unique substrate preference; the enzymes directly reduce hydroperoxidized phospholipids integrated into membranes (Ursini and Bindoli, 1987). Members of the other GPx families, however, interfere with

* Corresponding author: Department of Molecular Parasitology, Sungkyunkwan University School of Medicine, 300 Cheoncheon-dong, Suwon, Gyeonggi-do 440-746, Korea. Tel: +82 31 299 6261. Fax: +82 31 299 6269. E-mail: ykong@med.skku.ac.kr
† These authors contributed equally to the work.
§ Present affiliation: Department of Parasitology, School of Medicine, Wuhan University, Wuhan 430071, China.

doi:10.1017/S0031182009005654 Printed in the United Kingdom

lipid peroxidation only via a concerted operation with phospholipase (Grossmann and Wendel, 1983), which implies that PHGPxs are deeply associated with the repair of disrupted biomembranes (Imai and Nakagawa, 2003). GPxs might also constitute the front line of enzymatic defence to ensure their survival against host immune cell-derived ROS in parasitic helminthes, which cause chronic infections (Cookson *et al*. 1992; Zelck and von Janowsky, 2004). The helminth GPx families show a certain degree of biased distribution across taxa. GPx proteins homologous to mammalian GPx3 (plasma GPx) have been characterized in the filarial nematodes including *Brugia pahangi*, *Dirofilaria immitis* and *Wuchereria bancrofti* (Henkle-Dührsen and Kampkötter, 2001); while information on the GPx4 members is obtainable from trematode species such as *Schistosoma mansoni* and *Clonorchis sinensis* (Williams *et al*. 1992; Mei and LoVerde, 1995; Cai *et al*. 2008).

Paragonimus westermani is a parasitic trematode, which causes inflammatory lung granuloma, as well as systemic infections in Asian, American and African countries (WHO, 1995). Consumption of raw or undercooked crustaceans or wild boar infected with the metacercariae has been the principal route for human infection (WHO, 1995; Blair *et al*. 1999). After being ingested, the metacercariae excyst within the duodenum, migrate through the peritoneal cavity and finally arrive in the lungs, where they mature. The adult worms are surrounded by thick fibrous granulomatous cyst, in which infiltration of inflammatory phagocytes generating various reactive radicals prevail (Nakamura-Uchiyama *et al*. 2002). The high oxygen tension of the lungs may also be a primary factor in the creation of a hostile host environment (Comhair and Erzurum, 2005). In order to overcome these stressful conditions and to maintain its life-span, the fluke is equipped with several antioxidant enzymes, including peroxidase, superoxide dismutase (SOD) and glutathione S transferase (GST) (Chung *et al*. 1992; Hong *et al*. 2000; Li *et al*. 2005).

In this study, we isolated and characterized 2 novel genes encoding GPx from the human lung fluke. Expression of the *PwGPx1* gene increased gradually in accordance with the development of the parasite, whereas that of *PwGPx2* maintained at the basal level from the metacercaria to the 3-week-old juvenile, and peaked in the egg-laying stage. The *Paragonimus* proteins localized specifically in vitellocytes within vitelline glands and eggs. *In vitro* experiments demonstrated that oxidative stress-inducible chemicals such as paraquat, juglone and H_2O_2 substantially augmented the expression of *PwGPx1* and *PwGPx2* in viable worms. The PwGPx proteins might actively participate in the detoxification of oxidative damage during egg production. Our results further suggest their physiological implications during the parasite's adaptation in hostile host environments.

MATERIALS AND METHODS

Parasite, DNA and RNA samples

Dogs were orally infected with 200 metacercariae of either diploid- or triploid-type *P. westermani*, which were collected from naturally infected crayfish, *Cambaroides similis*. The 1- and 3-week-old juveniles were harvested from the peritoneal cavity, and the 7- and 12-week-old worms were obtained from the lungs. The worms were washed >10 times with physiological saline at 4 °C. A total of 20 adult worms (12-week-old) were incubated overnight in physiological saline, and the eggs were isolated and cleaned under a dissecting microscope (purity >99%). The triploid worms were used as the principal experimental material in this study, with an exception of the genomic DNA employed in Southern blotting. The use of experimental animals was approved by the Animal Ethics Committee of the Korea Food and Drug Administration (protocol number NIH-05-09). Total RNA and DNA samples were prepared using TRIzol reagents (Invitrogen, Carlsbad, CA, USA) and the Wizard Genomic DNA Purification Kit (Promega, Madison, WI, USA).

Analysis of expressed sequence tag (EST) and cDNA library screening

The nucleotide sequences of lambda clones randomly selected from a *P. westermani* cDNA library were analysed against the non-redundant databases of nucleotide and protein sequences at the National Center for Biotechnology Information (NCBI, http://www.ncbi.nlm.nih.gov), using BLAST algorithms. EST-1 (designated *PwGPx1*) and EST-34 (*PwGPx2*), which revealed significant matches with the *GPx* genes of other organisms, were selected for further characterization. The cDNA library was screened by standard plaque lift hybridization using each of the DNA fragments as a probe. The insert cDNAs from positive clones were amplified by PCR using the universal T3 and T7 promoter primers, cloned into pMD18-T vector (Takara, Shiga, Japan) and subjected to nucleotide sequencing from both strands to obtain a full-length cDNA encompassing each of the ESTs. The coding profiles and homology patterns of the cDNAs were analysed using the ORF Finder and BLAST programs implemented in the NCBI server. The selenocysteine (Sec) insertion sequence (SECIS) motif was predicted using the SECISearch program (ver2.19; http://genome.unl.edu/SECISearch.html). The putative hydrophobic signal peptide was predicted by the SignalP program (http://www.cbs.dtu.dk/services/SignalP). The ScanSite pI/Mw program (http://scansite.mit.edu/calc_mw_pi.html) was used to calculate the theoretical molecular weights (Mr) and isoelectric point (pI).

https://doi.org/10.1017/S0031182009005654 Published online by Cambridge University Press

Amplification of the chromosomal PwGPx *gene segments and Southern blot analysis*

The entire gene segments corresponding to *PwGPx1* and *PwGPx2* were amplified from the *P. westermani* genome by long-range PCR using gene-specific primer pairs, which were designed from the nucleotide sequences within both ends of each cDNA (5′-GGTACCAACAGTGACGGTTTGATTTTCT-AACACC-3′ and 5′-GACAGGCCTGGAGGTG-AATTGA TGAGAGTGAACC-3′ for *PwGPx1*; 5′-GGAACATCGAAGGTGGTTTGAAAAAG-GTCAACTTC-3′ and 5′-CTTTACTCACAAAC-TACT GTTGCAATAATAGTAACGTC-3′ for *PwGPx2*). PCR was conducted with the LA *Taq* system (Takara), after which the PCR products were cloned into the pGEM-T Easy vector (Promega) for sequencing.

The genomic distributions of *PwGPx*s were determined by Southern blotting. The DNA probes were prepared by PCR using plasmids containing each of the full-length genes and specific primers matched to the 3′-region of each gene (5′-CAC-CGTCACAGCATTTCTCATTTC-3′ and 5′-CT-GCTGAACAAAATATGCATG-3′ for *PwGPx1*; 5′-GGCTAACAATAGACTTTTGTAC-3′ and 5′-CTTTACTCACAAACTACTGTTGC-3′ for *PwGPx2*). During amplification, the amplicons were labelled with digoxigenin (DIG; PCR DIG Probe Synthesis Kit, Roche Applied Science, Mannheim, Germany). The genomic DNAs (10 μg each) of the diploid and triploid worms were digested with *Bam*H I (one cutting site within the *PwGPx1* probe, and none within the *PwGPx2* probe), resolved on 0·8% agarose gels and blotted onto Hybond-N membranes (Amersham Pharmacia, Uppsala, Sweden). The membranes were hybridized overnight with the DNA probes. After washing the membranes under high-stringency conditions (0·1 × SSC), the positive signals were detected with a Dig Luminescent Detection Kit (Roche Applied Science).

Phylogenetic analysis

The translated amino acid (aa) sequences of *PwGPx1* and *PwGPx2* were used as queries in a series of BLAST searches, to retrieve the closely matched sequences from a variety of GenBank genomic databases. The aa sequences of both human cytosolic (GPx1, CAA68491) and plasma (GPx3, AAP50261) GPxs, and *B. pahangi* GPx (GPx3 lineage, CAA48882) were also employed as other queries during the BLAST searches. The aa sequences were aligned with ClustalX and optimized using the GeneDoc program. A phylogenetic analysis was conducted with the sequence alignment by neighbor-joining algorithm, using the NEIGHBOR program in the PHYLIP package (ver3.6b). The tree was displayed with TreeView and the statistical significance of each of the branching points was evaluated using 100 random samplings of the input alignment, by the SEQBOOT program.

Semi-quantitative reverse transcription-PCR (RT-PCR)

The mRNA transcripts of the *PwGPx1* and *PwGPx2* genes were detected from the total RNAs extracted from various developmental stages of *P. westermani*, including egg, metacercaria, juvenile and adult worm. Each of the transcripts was reverse-transcribed into the single-strand cDNAs using a RNA PCR kit (AMV, ver2.1; Takara) and a gene-specific reverse primer (5′-TTAGGGGCCAAGC-ATTTTGTAAATAC-3′ for *PwGPx1* and 5′-CT-ATTGACTCAACATTCGTTGAATGC-3′ for *PwGPx2*), and then amplified by adding a forward primer into the reactants in the following PCR (5′-ATGCGAAAGCTTTTTGCTTTGTTGTTC-3′ for *PwGPx1* and 5′-ATGGGGAGCTCATTTG-GGCTGCTC-3′ for *PwGPx2*). The PCRs were conducted with a thermal cycling profile of 94 °C for 4 min, 25 cycles of 50 sec at 94 °C, 40 sec at 60 °C, 1 min at 72 °C and a final extension of 10 min at 72 °C. The number of amplification cycles was empirically determined by preliminary PCRs to ensure that the product is produced from the exponential phase of each amplification reaction. The reaction products were resolved by 2% agarose gel electrophoresis and visualized by ethidium bromide staining. A primer pair of the β-*actin* gene (5′-GGCCATGTACGTTGCTATCC-3′ and 5′-CA-GAGAGAACAGTGTTGGCG-3′) was utilized in reactions for quantity control, and the absence of any contaminating chromosomal DNA was verified via the preparation of reactions without reverse transcriptase during the first round of cDNA synthesis.

Cloning, expression and antibody production

The open reading frame (ORF) regions of *PwGPx*s were amplified by PCR from the positive cDNA library clones as described above, and cloned into pGEM-T Easy vector. The unusual Sec codon (TGA) of *PwGPx2* was converted into the standard Cys codon (TGC), by using a complementary primer pair (5′-CATCCAACTGCGGTCTGGCAGAT-TTAAATTACC-3′ and 5′-GGTAATTTAAA-TCTGCCAGACCGCAGTTGGATG-3′) and the QuikChange Site-Directed Mutagenesis Kit (Stratagene, La Jolla, CA, USA). The plasmids were transformed into competent *Escherichia coli* DH5α cells and the nucleotide sequences were confirmed by sequencing.

Nucleotides corresponding to the mature domains of PwGPxs were amplified from each of the plasmid constructs using primers containing restriction

https://doi.org/10.1017/S0031182009005654 Published online by Cambridge University Press

sites for *Eco*R I and *Xho* I (5′-AAGAATTCT-TGCCTAACCAA CGACCGTCTCATG-3′ and 5′-CCCTCGAGTTAGGGGCCAAGCATTT-TGTAAATA-3′ for *PwGPx1*; 5′-AAGAATTC-CTCCCAAATAGGGACGCTGATTC-3′ and 5′-CCCTCGAGCTATTGACTCAACATTCGT-TGAATG-3′ for *PwGPx2*). Amplicons were purified with a QIAquick PCR Purification Kit (Qiagen, Valencia, CA, USA), and digested with the corresponding enzymes. The DNAs were cloned into the pET-28a-c(+) vector (Novagen, Madison, WI, USA), transformed into *E. coli* DH5α cells and the accuracy of the nucleotide sequences was verified by sequencing. The plasmid DNAs harbouring the correct codons were introduced into *E. coli* BL21 (DE3) cells. Expressions of the recombinant proteins were induced with 0·5 mM isopropyl-β-D-thiogalactopyranoside (IPTG). The bacterial cells were sonicated and the recombinant proteins were purified using Ni-NTA agarose column (Amersham Biosciences). The purified recombinant PwGPx (rPwGPx) proteins were analysed by 12% SDS-PAGE and used to generate specific antibodies.

Six-week-old, specific pathogen-free female BALB/*c* mice were immunized subcutaneously 3 times (2-week interval) with the purified rPwGPxs (30 μg each) mixed with Freund's adjuvant (Sigma). The final booster was done with 10 μg proteins through the intravenous route. One week after the final injection, blood was collected by heart puncture. The blood was centrifuged for 10 min at 3000 ***g*** at 4 °C and the antisera were stored at −70 °C until use.

Two-dimensional (2-D) SDS-PAGE and Western blotting

P. westermani adult worms were homogenized with cold physiological saline (PBS; 50 mM, pH 7·2) containing a protease inhibitor cocktail (Roche). The homogenate was subjected to centrifugation for 30 min at 20 000 ***g*** at 4 °C, and the supernatant was used as a crude extract. For 2-D electrophoresis, the crude extract (50 μg) was precipitated with ice-chilled 20% TCA, and washed twice in cold acetone prior to air-drying in a SpeedVac (Savant, Holbrook, NY, USA). The sample was mixed with rehydration buffer, loaded to an IPG strip (pH 3–10) using a cup-loading instrument on an IPGphor system (Amersham Biosciences) and focused for a total of 35 kVh. Subsequent 2-D electrophoresis was done on 12% SDS-PAGE gels (160 × 160 × 1 mm). The proteins were stained with colloidal Coomassie Blue G-250 (CBB), or processed further with immunoblotting against either the rPwGPx1- or rPwGPx2-specific mouse antiserum. Proteins separated by 2-D SDS-PAGE were transferred onto nitrocellulose membranes (Schleicher & Schuell BioScience, Dassel, Germany). The membranes were blocked for 1 h with Tris-buffered saline containing 0·05% Tween-20 (TBS/T) and 5% skim milk, followed by overnight incubation with rPwGPx-specific antiserum diluted to 1 : 3000 in TBS/T containing 5% skim milk at 4 °C. The membranes were incubated for 1 h with peroxidase-conjugated goat anti-mouse IgG antibody (1 : 4000 dilution; Cappel, West Chester, PA, USA). The signals were detected with an ECL detection system (Amersham Biosciences).

Purification and enzyme kinetics of PwGPx1 and PwGPx2

Native PwGPx proteins were purified from the adult worm extract employing AKTA fast-performance liquid chromatography on 1·6 × 60 cm-long Superdex 75 gel filtration followed by DEAE-anion exchange chromatography (2·6 × 15 cm-long; Amersham Pharmacia Biotech, Uppsala, Sweden), monitoring their enzyme activities. The purified GPx proteins were dialysed against PBS (pH 7·2) overnight at 4 °C.

The specific enzyme activity was examined by the reduction of H_2O_2 or cumen hydroperoxide (Sigma-Aldrich) in the presence of GSH and *E. coli* glutathione reductase (GR). The 200 μl reaction mixture contained 5 mM potassium phosphate, 1 mM GSH, 0·1 unit of GR, 0·1 mM NADPH and 1 mM EDTA. The reagents were pre-warmed to room temperature just prior to use in the reaction. After adding the substrate, levels of NADPH oxidation were monitored at 340 nm (A_{340}) for 5 min with a spectrophotometer. A steady-state kinetic assay was performed in the same manner by increasing the amount of each substrate. K_m and V_{max} values were determined using the Enzyme Kinetics Module (ver 1.3) integrated into SigmaPlot (ver 10.0.1; Systat Softmare, San Jose, CA, USA).

Induction of P. westermani GPxs *under the oxidative stresses*

A total of 35 viable adult worms were pre-incubated in 50 ml of RPMI 1640 medium for 1 h at 37 °C, then transferred to fresh RPMI medium (5 worms per experimental group) supplemented with methyl viologen dichloride hydrate (paraquat; 25 and 100 mM, Sigma), 5-hydroxy-1,4-naphthoquinone (juglone; 25 and 100 μM, Sigma) or H_2O_2 (0·5 and 2 mM). The worms were incubated for 1 h at 37 °C, after which total RNAs were extracted immediately as described above. The relative amounts of the *PwGPx* transcripts were estimated by semi-quantitative RT-PCR, as described above. In addition, the other antioxidant enzymes of *P. westermani* were included in this experiment as a comparative group. The selected genes and their specific primer pairs were as follows: *Cu/Zn-SOD* (AY675506), 5′-ATGA-AGGCTGTTTGTGTCCTTAC-3′ and 5′-CTA-TTCTGACCAACCAATCAC-3′; *GST28* (L43919), 5′-ATGTCGACCCCGAAGTATAAG-3′ and

https://doi.org/10.1017/S0031182009005654 Published online by Cambridge University Press

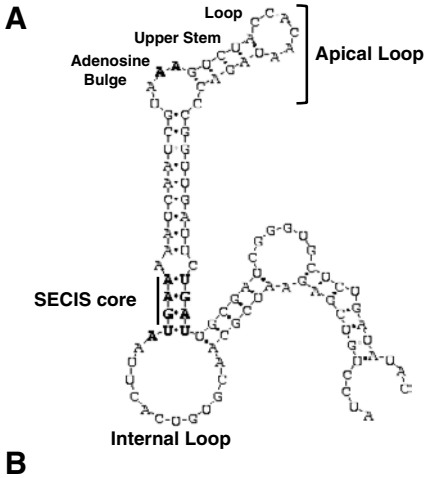

B

Organism	GenBank Number	Helix I →	Internal loop	Quarter (SECIS core)	Helix II →	Apical loop	Helix II ←	Quarter (SECIS core)	Internal loop	Helix I ←
P. westermani	**DQ454160**	AUCGC	ACG//UUA	**A UGAA**	AAA//UCG	**AA** GUCUACCACA	CGG//UUC	**UGAU**	U	GCGAU
S. mansoni	M86510	ACAAA	UUC//UAU	**A UGAC**	GAU//CUC	**AA** AUGUUCAUU	GUC//GGU	**UGAU**	GAA//AGU	UUUGU
H. sapiens	X71973	GCC	ACUC	**A UGAC**	GGC//UGC	**AA** ACCU	GCU//GGC	**AGAC**	CCG//CAG	GGC
M. musculus	D87896	GCC	ACUC	**A UGAA**	GGU//UGA	**AA** ACC//GUG	GGG//UCC	**UGAG**	GACCU	GGC
S. scrofa	X76009	GUGCC	CC	**A UGAC**	AGU//UAA	**AA** ACC//GUG	GGG//ACU	**CGAG**	AACC	GGCAC

Fig. 1. Analysis of selenocysteine insertion sequence (SECIS) motif in *PwGPx2* of *Paragonimus westermani*. (A) The secondary structure SECIS found in the 3′-untranslated region (UTR) of *PwGPx2* mRNA. The structure was determined by using the SECISearch program. (B) The primary structures of the SECIS motif. Nucleotide sequences constituting the 3′-UTR SECIS motifs were retrieved from the phospholipid hydroperoxide glutathione peroxidase genes of *P. westermani*, *Schistosoma mansoni*, *Homo sapiens*, *Mus musculus* and *Sus scrofa*, and aligned in accordance with the predicted secondary elements. Nucleotides conserved within the invariant SECIS core (Quarter) and apical loop are highlighted by boldface letters.

5′-TCAGAGGTCCGTTGTAGGCC-3′. The PCR products were resolved by 2% agarose gel electrophoresis together with standards for quantification. The relative transcription levels of each gene were digitalized by measuring their intensities with the LAS-1000plus system and the MultiGauge Program (ver3.0; FUJIFILM, Tokyo, Japan). These values were normalized against those of the *β-actin* gene, which was employed as an internal control. The fold inductions of the selected genes were calculated by comparing the values between experimental and control reactions.

Immunohistochemical localization

Fresh adult worms were fixed overnight in PBS containing 4% paraformaldehyde at 4 °C. The worms were dehydrated with a graded ethanol series and embedded in paraffin blocks. Sections (4 μm-thickness) were mounted on microscope slides, deparaffinized, rehydrated and rinsed with PBS. The sections were treated with 3% hydrogen peroxide (5 min), followed by blocking with 1% BSA (1 h). The sections were incubated overnight with the anti-rPwGPx1 or anti-rPwGPx2 mouse antibodies diluted to 1 : 200 in PBS supplemented with 1% BSA at 4 °C. The reactions were visualized with a horseradish peroxidase-conjugated anti-mouse IgG rabbit antibody (1 : 500) and diaminobenzidine under the manufacturer's instruction (Roche). Pre-immune mouse serum diluted to the same ratio was employed as a control. The slides were observed under a light microscope (Axioplot, Carl Zeiss, Jena, Germany).

RESULTS

Isolation of P. westermani *genes putatively encoding GPx*

By analysing randomly selected EST clones of the *P. westermani* adult, we obtained 2 clones (Pw-EST-1, 601 bp-long; Pw-EST-34, 643 bp-long), of which deduced aa sequences shared significant identities with those of GPxs isolated from a variety of organisms, including *S. mansoni* (AAU34080 and AAC14468), *C. sinensis* (ABK58679, ABK58680, ABK58681 and ABK58682), *Aedes aegypti* (AAQ02888), *Mus musculus* (BAA22780) and human (CAA50793) (*E*-values $< 3 \times 10^{-23}$). The complete cDNA sequences encompassing each of the clones were determined by consecutive cDNA library screening using the EST clones as probes. The cDNAs, designated *PwGPx1* and *PwGPx2* (*Paragonimus westermani* glutathione peroxidase), were comprised of 971 and 918 bp, and contained each single ORF of 189 and 192 codons, from an ATG at nucleotide positions 67–69 and 41–43 to a TAA/TAG at positions 633–635 and 616–618, respectively. In addition to the conventional stop codon, *PwGPx2* harboured the second TGA codon within its ORF (nucleotide positions at 233–235), which might

https://doi.org/10.1017/S0031182009005654 Published online by Cambridge University Press

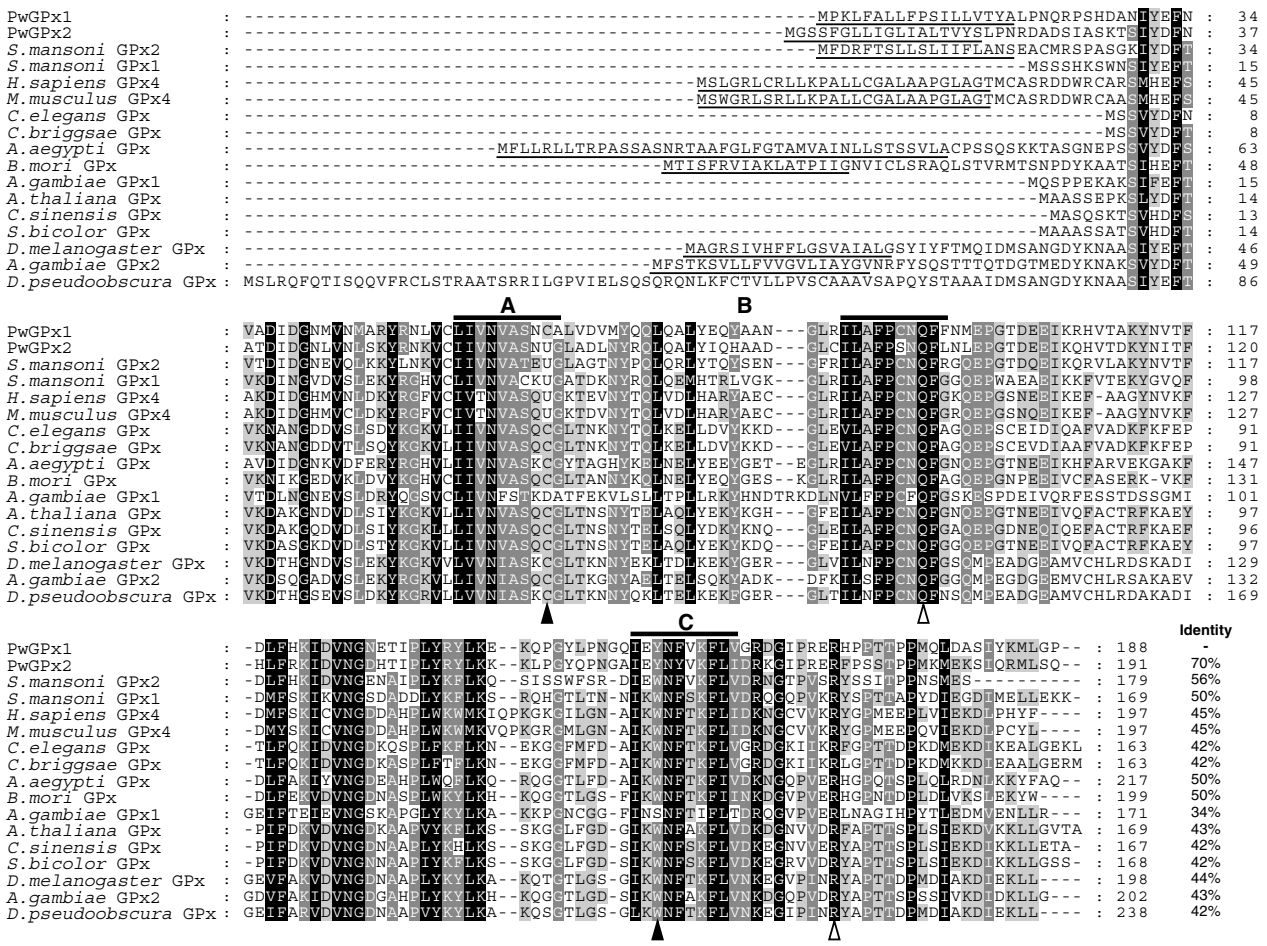

Fig. 2. Multiple sequence alignment of PwGPxs with other phospholipid hydroperoxide glutathione peroxidase (PHGPx) members. The deduced amino acid sequences of PwGPx1 and PwGPx2 were aligned with those of *Schistosoma mansoni* (AAU34080 and AAC14468), *Homo sapiens* (CAA50793), *Mus musculus* (BAA22780), *Caenorhabditis elegans* (CAB03004), *Caenorhabditis briggsae* (CAE60228), *Aedes aegypti* (AAQ02888), *Bombyx mori* (BAE07196), *Drosophila melanogaster* (AAR96123), *Drosophila pseudoobscura* (EAL29978), *Anopheles gambiae* (XP_313166 and XP_313168), *Arabidopsis thaliana* (CAB78203), *Citrus sinensis* (CAE46896) and *Sorghum bicolor* (AAT42166), employing the Clustal X program, then optimized with GeneDoc. The identical amino acids in the alignment are highlighted in black, while similar residues are shown in grey. Three well-conserved domains found in the members of PHGPx are indicated by solid bars with A, B and C. The functional amino acid residues engaged either in the formation of the catalytic centre or in the binding of the glutathione molecule are marked with filled and open arrowheads, respectively. The abbreviation 'U' in functional domain A represents selenocysteine. The putative signal peptides are underlined. The identity value of each enzyme against PwGPx1, which was calculated from the alignment after removing positions with a gap as missing data, is provided at the end of the alignment.

decode the 21st aa, Sec (Stadtman, 1996). In association with the presence of the opal codon, a SECIS motif was detected at nucleotide positions 673–775 within the 3′-untranslated region (UTR) (Fig. 1). The sequence conserved several structural motifs, including 2 helices separated by an internal loop, a SECIS core structure, a quartet located at the base of the second helix and an apical loop; all of which have been well described in a series of *GPx* genes (Kryukov *et al*. 2003). In contrast, *PwGPx1* contained a standard codon for cysteine (TGC), rather than the Sec codon at the corresponding position and the SECIS was not screened within its nucleotide sequence. Nucleotide sequences of *PwGPx1* and *PwGPx2* were registered in the GenBank under Accession nos. DQ454159 and DQ454160.

Determination of primary structures of PwGPx1 and PwGPx2

The polypeptides encoded by *PwGPx1* (188 aa) and *PwGPx2* (191 aa) harboured the predicted molecular masses of 21·7 and 21·6 kDa, respectively, and shared a considerable degree of sequence identity with one another (70%, Fig. 2). The 18 aa residues encompassing the N-terminus of these polypeptides

https://doi.org/10.1017/S0031182009005654 Published online by Cambridge University Press

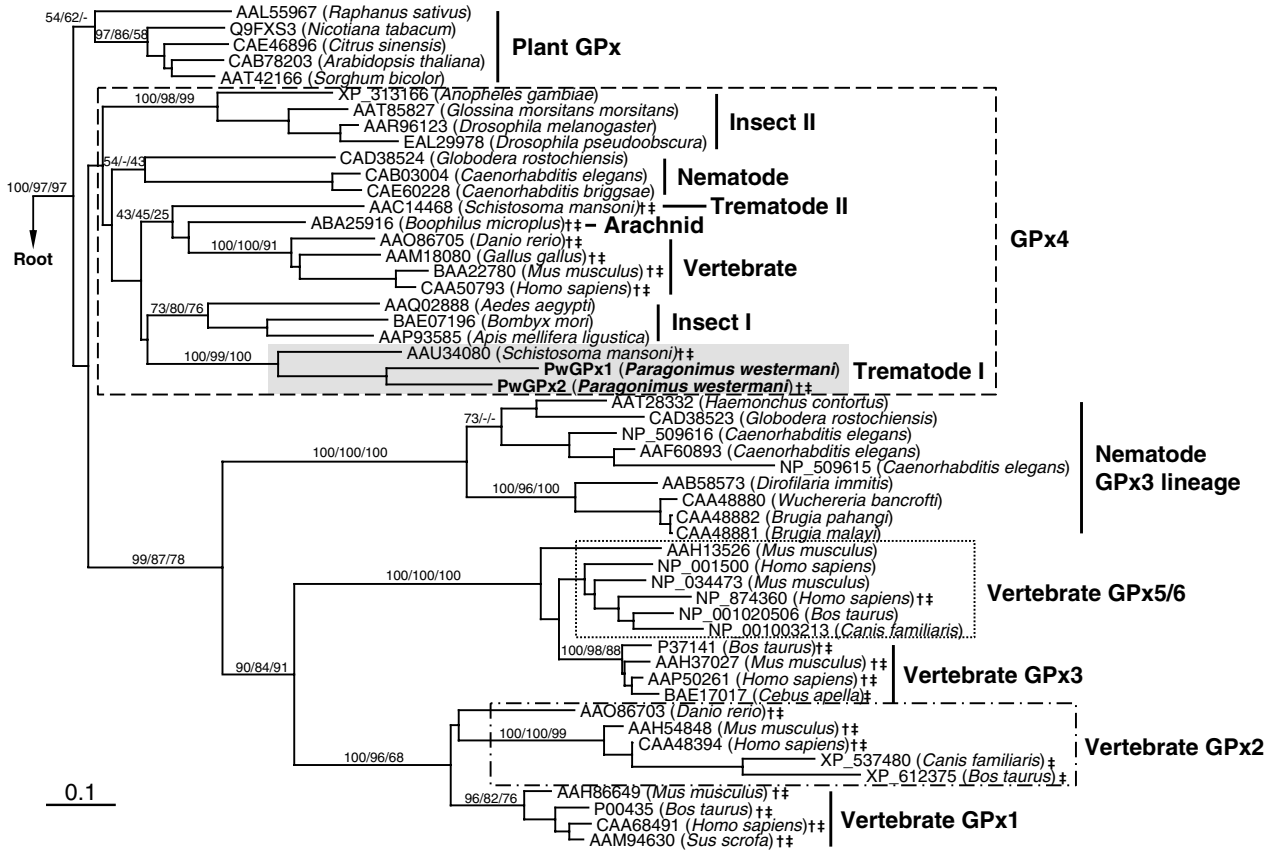

Fig. 3. The evolutionary relationships of the *PwGPx* genes with members of the various *GPx* gene families. The phylogenetic positions of *PwGPx1* and *PwGPx2* were predicted on the basis of alignment of amino acid sequences. The tree was constructed by a neighbor-joining algorithm using PHYLIP and was rooted with GPxs of *Neurospora crassa* (CAE76176) and *Saccharomyces cerevisiae* (NP_009803). Numbers at the major branching nodes indicate their percentages of appearance in 100 bootstrap replicates, and values obtained from other analyses using either maximum parsimony or maximum likelihood algorithms are also presented to ensure the statistical significance of these nodes. The identity of each analysed sequence is distinguished by a protein identification number, followed by the species name from which it was isolated. The presence of selenocysteine (Sec) codon (†) and Sec insertion sequence (‡) within corresponding mRNA sequence is indicated at the end of each sequence identity.

were found to be hydrophobic and predicted as target signals for the translocation of the proteins (underlined sequences in Fig. 2). The Trp residue forming a hydrogen bond with the reactive Sec was replaced by Tyr, another aa with an aromatic side-chain, in the *Paragonimus* homologues (filled arrowhead in domain C, Fig. 2). Among the 3 aa residues involved in the formation of a salt bridge and hydrogen bond to the glutathione molecule (Epp *et al*. 1983), only the Gln and downstream Arg residues were shown to be tightly conserved among members of PHGPx, including PwGPxs (open arrowheads in Fig. 2). The aa block, which was associated with a tetrameric structure in mammalian GPx proteins other than PHGPxs, was not detected in the aa sequences of PwGPxs (data not shown).

Phylogenetic relationships of PwGPxs with their homologues

We used the aa sequences of PwGPx1 and PwGPx2 in homology searches with BLAST algorithms and found several hundred entries from the GenBank database. These sequences revealed various degrees of sequence identity ranging 35%–53% (*E*-values $<10^{-16}$), of which the majority were PHGPx-like proteins. Information regarding the other GPx families was obtained by a series of subsequent BLAST searches using the aa sequences of human and nematode GPx3. A total of 52 members were finally selected, by considering both the identity values and taxonomical distributions and used in a phylogenetic analysis. In the neighbor-joining tree, the GPxs of higher vertebrates including human and mouse were separately categorized into the 6 GPx families (Fig. 3). With the plant GPxs, proteins isolated from invertebrate animals, much closer relationships with the mammalian PHGPxs were shown, which was consistent with the results of the structural comparison (Fig. 2). However, nematode species were found to express both of the GPx lineages (GPx3 and GPx4). The screenings of the draft genomic sequences of *S. mansoni* (assembly version 3 at the Sanger Institute) and *Anopheles gambiae*

https://doi.org/10.1017/S0031182009005654 Published online by Cambridge University Press

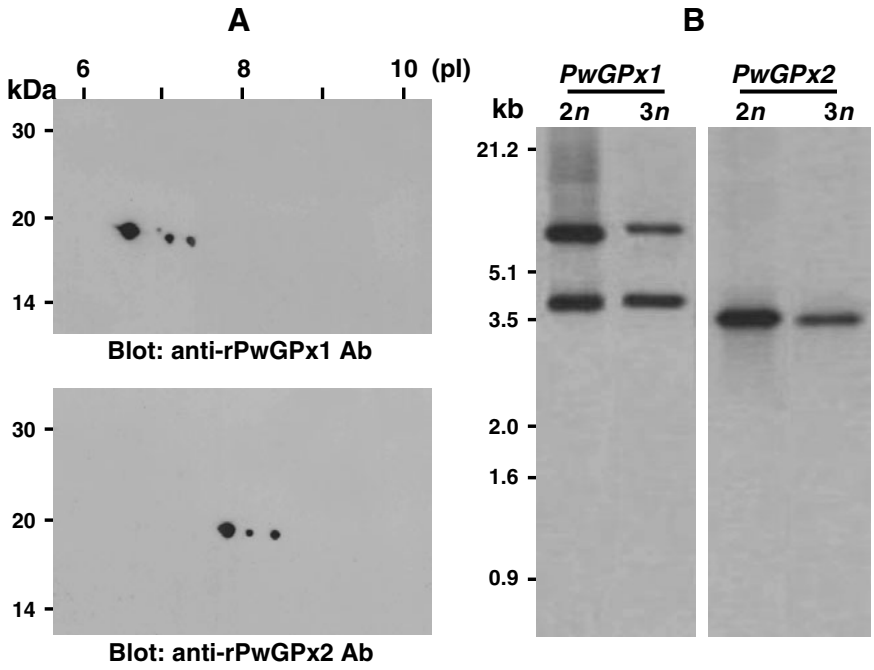

Fig. 4. Expression and genomic distributions of the *PwGPx* genes. (A) Two-dimensional (2-D) Western blots of PwGPx1 and PwGPx2. The adult crude extract (50 μg) was isoelectrically focused using IPGphore (pH 3–10), and further resolved by 12% SDS-PAGE. Separated proteins were transferred onto nitrocellulose membranes, and probed with the rPwGPx1- and rPwGPx2-specific mouse antisera (1 : 3000 dilution), respectively. Molecular mass in kDa and isoelectric points (pI) are shown on the left and top. (B) Southern blot analyses of *PwGPx1* and *PwGPx2*. The genomic DNAs (each of 10 μg) of both diploid (2*n*) and triploid (3*n*) *Paragonimus westermani* were digested with *Bam*H I (one cut in *PwGPx1* but no cut in *PwGPx2* probes) and probed with digoxigenin-labelled gene-specific DNA fragments. The positions of the DNA size standards (in kb) are also shown.

(NCBI database) showed no evidence reflecting the presence of *GPx1/GPx3*-like genes in these genomes (data not shown). The tree also revealed that each of the trematode and insect PHGPxs had diverged separately into 2 distinct subclades. In addition to the biased distributions of GPx families, the Sec codon and the associated SECIS motif were recognized largely within the mRNA sequences coding for the trematode and vertebrate GPx members (indicated by † and ‡, respectively, in Fig. 3). Among the arthropod proteins examined, only an arachnidal PHGPx (*Boophilus microplus*, ABA25916) was found to be Sec-dependent.

Genomic distribution of PwGPxs *and expression of native PwGPx1 and PwGPx2 proteins*

As shown in Fig. 4A, the 3 protein spots, which migrated at approximately 20 kDa, were detected to be strongly reactive against each of the rPwGPx-specific antibodies by the 2-D Western blot analyses of an adult worm extract. The average pI values of the reactive spots were comparable to that of either PwGPx1 (6·04) or PwGPx2 (8·37), which had been predicted theoretically from the deduced aa sequences. In order to determine whether these spots represented paralogues or allelic forms, Southern blot analyses of *PwGPx1* and *PwGPx2* were carried out with the genomic DNAs from both diploid (2*n*) and triploid (3*n*) worms digested with the restriction enzyme, *Bam*H I. The enzyme harboured a single cut in *PwGPx1* but no cut in *PwGPx2*. The *PwGPx1* probe revealed 2 signal bands with nearly identical intensity, while that of PwGPx2 detected a single band (Fig. 4B). This result showed that the *PwGPx1* and *PwGPx2* might exist as a single copy gene in the parasite genome. Therefore, the multiple spots identified by Western blotting seemed to represent the major allelic forms of *PwGPx1* and *PwGPx2*, with considerable frequencies in the *P. westermani* population. The nucleotide sequences acquired from the cDNA library revealed 3 representative alleles of the *PwGPx2* gene (unpublished observation). The pI values of these alleles could be differently calculated as 7·86 (68·3%), 8·31 (12·2%) and 8·37 (14·6%), due to diagnostic base substitutions introduced within their sequences. These values appeared to match well with those of positive spots in the Western blotting. The cDNA sequences corresponding to *PwGPx1* also showed a matching pattern similar to that of *PwGPx2*. Any protein homologous to PwGPx1 or PwGPx2 was not detected in the excretory-secretory products of the parasite, which further suggested that the N-terminal hydrophobic sequences are responsible for the targeting of the proteins into certain organelle(s),

https://doi.org/10.1017/S0031182009005654 Published online by Cambridge University Press

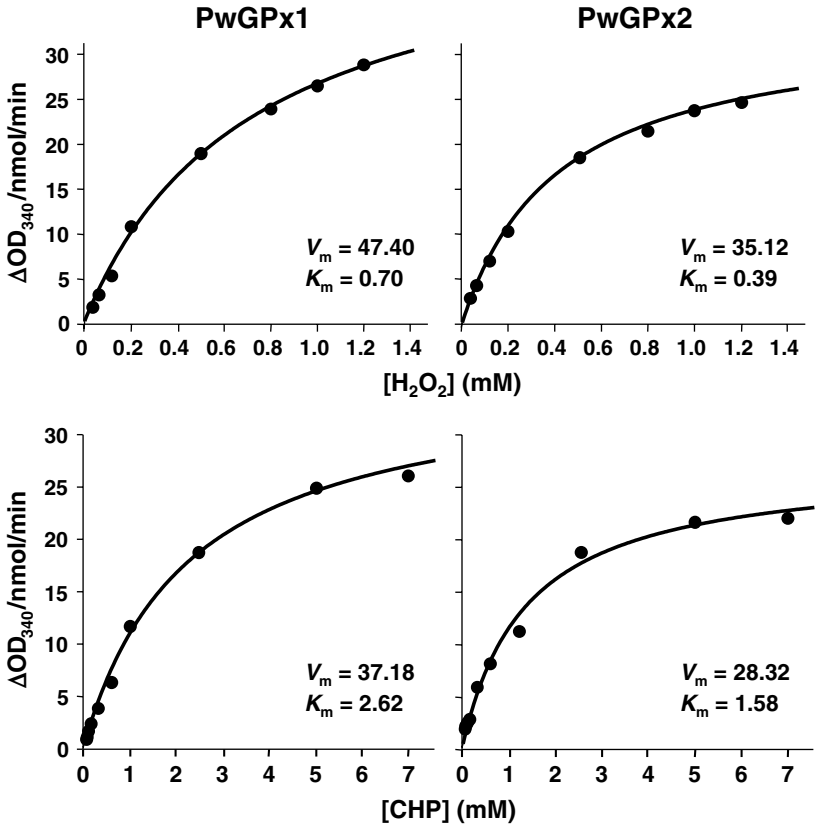

Fig. 5. Biochemical properties of native PwGPx1 and PwGPx2 proteins. The specificity and catalytic efficiency of the proteins purified by a series of gel chromatographies were examined toward catalytic substrates (H_2O_2 and cumene hydroperoxide [CHP]). The experiments were repeated 3 times and a representative result presented. The specific activity was calculated as ΔOD_{340}/nmol/min. The steady-state kinetics of the native proteins was analysed by measuring GPx activities using varying concentrations of the catalytic substrates and reduced glutathione. The V_{max} (V_m, ΔOD_{340}/nmol/min) and K_m (mM) values of each of the proteins are presented.

rather than into extracellular compartments (data not shown).

PwGPx proteins exhibited preferential substrate accessibility toward H_2O_2 rather than cumene hydroperoxide with an electron donor, GSH

We purified native PwGPx proteins though a series of column chromatographies since the recombinant forms of PwGPxs expressed in the *E. coli* cells did not show any detectable enzyme activity, probably due to lack of the post-translational phosphorylation process (Arthur, 2000). The purified enzymes efficiently reduced H_2O_2 and cumene hydroperoxide using GSH as an electron donor. The V_{max}/K_m ratios of PwGPx1 and PwGPx2 were determined to be 67·70 and 90·05, respectively, against H_2O_2, and 14·19 and 17·92, respectively, against cumene hydroperoxide (Fig. 5). These observations collectively suggested that PwGPxs possess preferential substrate accessibility toward H_2O_2 rather than cumene hydroperoxide, with GSH as an electron donor. The reducing potential of the Sec-dependent PwGPx2 was substantially higher than that of the Sec-independent PwGPx1 at the physiological pH.

Oxidative stress-inducible chemicals increased the expression levels of PwGPx1 *and* PwGPx2 *in viable worms*

We observed the induction patterns of the *PwGPx* genes by treating viable adult worms with oxidative stress-inducing chemicals such as paraquat, juglone and H_2O_2. As shown in Fig. 6, the worms incubated with 0·5 mM H_2O_2 demonstrated a highly up-regulated expression of *PwGPx1* (approximately 11-fold) and *PwGPx2* (4-fold). In addition, paraquat and juglone exerted their effects on the induction of these genes, although the extent was less than H_2O_2; an approximately 2–3 fold increase in *PwGPx1* and 1·5–2 fold increment in *PwGPx2* were observed. The transcription level of *Cu/Zn-SOD* was also increased in a manner comparable to that of *PwGPx2* upon stimulation, while that of *GST28* did not show significant elevation. High concentrations of H_2O_2 resulted in decreased expressions of these antioxidant

https://doi.org/10.1017/S0031182009005654 Published online by Cambridge University Press

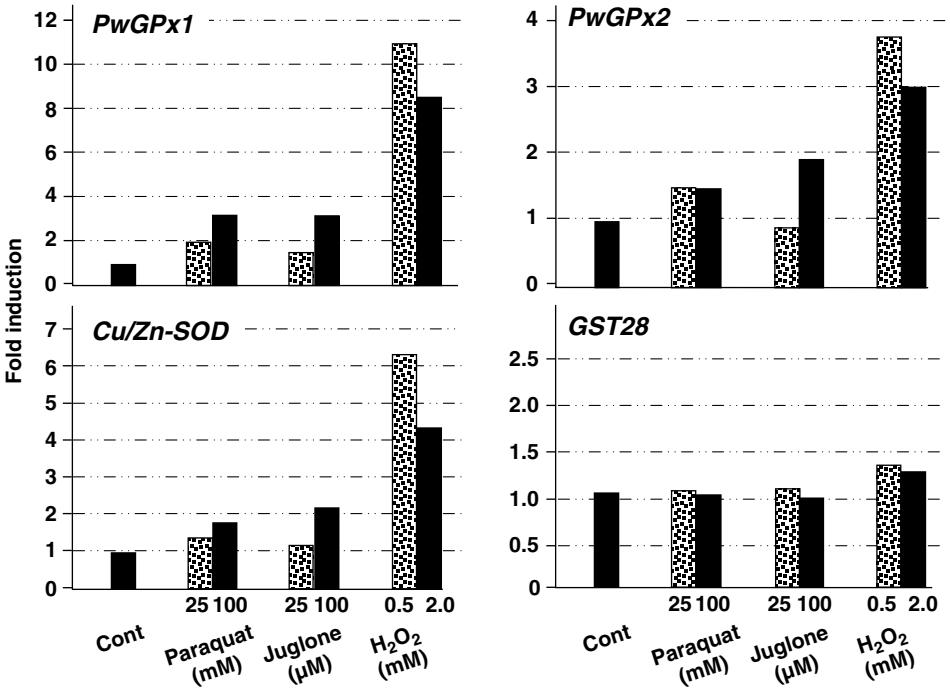

Fig. 6. Induction patterns of the *PwGPx* genes under oxidative stresses. Viable *Paragonimus westermani* adults were incubated for 1 h at 37 °C in RPMI 1640 medium supplemented with each of the indicated chemicals. The expression levels of *PwGPx1* and *PwGPx2* were determined by semi-quantitative RT-PCR. The relative amounts of the *PwGPx1* and *PwGPx2* transcripts were quantified via determination of the intensities of the electrophoresed amplicon bands. These values were normalized against those of the *β-actin* gene, which was employed as a quantity control (see Materials and Methods section). The fold inductions were calculated by comparing the intensities between each of the experimental and control groups. The transcription levels of the *Cu/Zn-SOD* (AY675506) and *GST28* (L43919) genes of *P. westermani* were also employed as comparative target genes. The reproducibility of the responsive inductions was examined by preparing the whole experimental batches 3 times, and a representative data set is shown in this figure.

genes, which might be attributable to a lethal effect of the chemical (30–40% death after treatment).

Expression pattern and localization of PwGPxs were highly associated with the maturation of reproduction-related cells

In trematode parasites, expressions of GPxs were increased proportionally according to the maturation and growth of the worm. The GPxs were shown to have specific localities within reproduction-related cells such as vitellocytes (Roche *et al*. 1996; Sayed *et al*. 2006; Cai *et al*. 2008). We observed the expressional regulation of the *PwGPx* genes in accordance with the developmental stages of *P. westermani* with the gene-specific primers via a semi-quantitative RT-PCR. The amplification of the target transcripts from total RNAs demonstrated that these genes are transcribed constitutively throughout all of the developmental stages examined, with different induction patterns. The transcription of *PwGPx2* was maintained at the basal level from the metacercariae to the 3-week-old juveniles, but the activity increased profoundly in the 7-week-old immature worms, and peaked in the 12-week-old adult worms and eggs. The expression of *PwGPx1* gradually increased during those developmental stages and reached its maximal levels at the egg-laying adult worm stage (Fig. 7A).

Tissue-specific distributions of PwGPx proteins were observed in adult worm sections employing anti-rPwGPx antibodies. As shown in Fig. 7B, immunohistochemical staining with the anti-rPwGPx1 antibody exhibited a strictly restricted localization pattern within the vitelline glands and intrauterine eggs. No positive reaction was detected in the other tissues or organs including ovary, seminal receptacle, testis, intestine and teguments. Antibody specific to the rPwGPx2 protein showed an immunoreactive pattern similar to that of the anti-rPwGPx1 antibody (data not shown).

DISCUSSION

The tissue-invasive helminth parasites may be continuously exposed to dual oxidative stresses, from both ROS generated by endogenous intracellular metabolism and ROS/nitric oxide generated by host inflammatory and immune cells (Selkirk *et al*. 1998; Zelck and von Janowsky, 2004). During their

https://doi.org/10.1017/S0031182009005654 Published online by Cambridge University Press

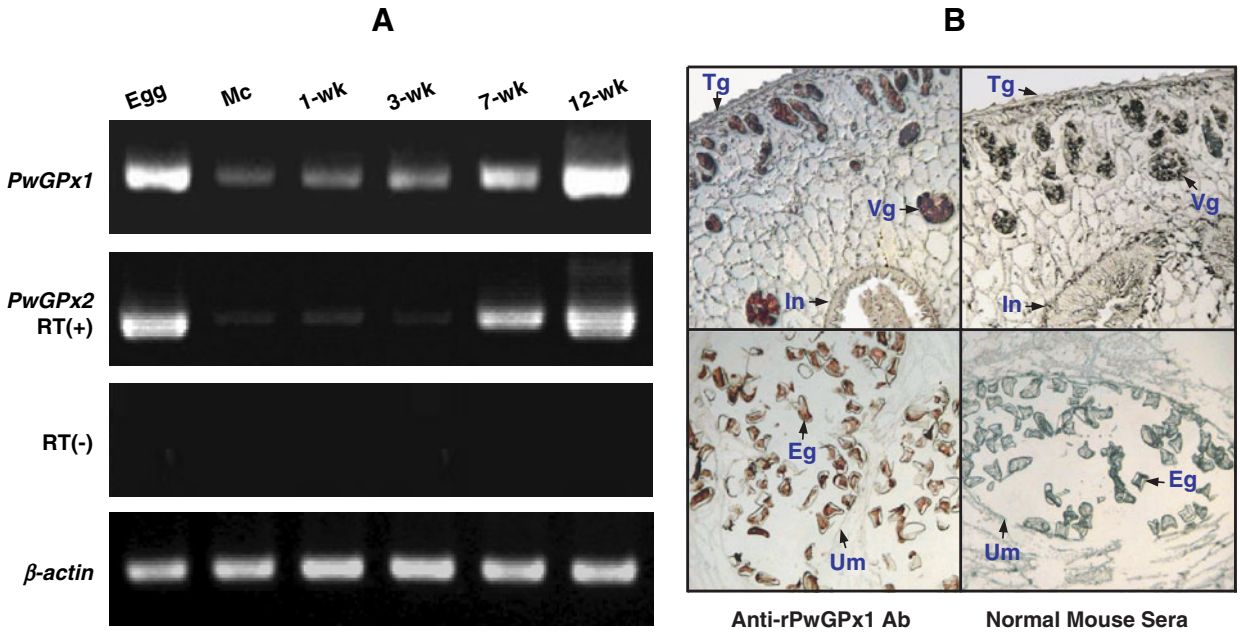

Fig. 7. Spatiotemporal expression of PwGPxs. (A) Expression profiles of *PwGPx1* and *PwGPx2* during the maturation of *Paragonimus westermani*. The transcription levels of *PwGPx1* and *PwGPx2* were examined with total RNAs extracted from the respective developmental stages as indicated on the top, via a semi-quantitative RT-PCR. The amplified products were separated on 2% agarose gels and stained with ethidium bromide. A primer pair for the *β-actin* gene was used as a quantity control. The absence of any contaminated genomic DNA was confirmed by preparing reactions without reverse transcriptase during the first round of cDNA synthesis (RT-). M, 100-bp DNA size standards; Mc, metacercaria. (B) Histological distribution of PwGPxs in *P. westermani* adult worm. Adult worm sections (4 μm thickness) were reacted with either the mouse antiserum specific to rPwGPx1 or with normal mouse serum (1 : 200 dilution). The positive signals are largely restricted within eggs and vitelline glands. Eg, eggs in uterus; In, intestine; Tg, tegument; Um, uterine membrane; Vg, vitelline glands.

life-span in host tissues, removal of ROS and protection of macromolecules from the oxidative attacks would be inevitable. The antioxidant enzymes might also constitute a major defensive system in these causative parasites (Callahan *et al*. 1988). Therefore, the helminths might be taken as a good model for investigation of the functional diversification with antioxidant enzymes. Together with the thioredoxin system, the glutathione-related molecules, such as glutathione, glutathione reductase, glutaredoxin and GPx, have been thought to perform crucial roles in thiol-disulfide redox homeostasis in these parasites, not only by providing electrons to essential enzymes but also by protecting them against oxidative stress (Henkle-Dührsen and Kampkötter, 2001; Salinas *et al*. 2004).

In the present study, we have isolated 2 novel genes that putatively coded for *P. westermani* GPxs. The deduced aa sequences of these genes revealed the primary structure characteristic to the PHGPx (GPx4) family, including aa conservation, absence of the subunit interaction domain and well-preserved catalytic and glutathione-binding domains. In a phylogenetic analysis, PwGPxs showed tight relationships with the other PHGPx-related members. PwGPx proteins preferred H_2O_2 as substrate rather than cumene hydroperoxide and an electron donor, GSH. Spatiotemporal expression of these proteins was highly associated with the maturation of reproduction-related cells. The up-regulated expression of PwGPxs induced by exogenous redox-recycling drugs and H_2O_2 suggested that these enzymes may actively participate in the detoxification of oxidative damage to protect *P. westermani* in high oxygen-tension status.

The general substrate affinity of GPx for H_2O_2 has been brought into question, as PHGPx shows a preference for lipid hydroperoxide. Furthermore, certain GPxs of parasitic nematodes have been examined to exhibit no enzymatic activity against H_2O_2 (Arthur, 2000; Henkle-Dührsen and Kampkötter, 2001). When we employed H_2O_2 as a principal substrate, a considerable level of specific GPx activity was detected in the *P. westermani* adult worm extract (data not shown). In addition, the treatment of viable worms with H_2O_2 induced significant up-regulation of *PwGPx1* and *PwGPx2* mRNA and protein expression. These results may suggest that trematodes, unlike the parasitic nematodes, are equipped with the GPx enzyme system, which directly functions as an H_2O_2 scavenger. Redox-cycling drugs such as juglone and paraquat are capable of crossing cell membranes and can be utilized as intracellular ROS inducers, as they trigger the conversion of oxygen into O_2^-

https://doi.org/10.1017/S0031182009005654 Published online by Cambridge University Press

(O'Brien, 1991). These chemicals also activated the *PwGPx* genes, albeit their effect was not as prominent as H_2O_2. The elevated GPx activity upon treatment of these drugs is likely to result indirectly from the accumulation of H_2O_2, via the action of SOD, and/or increased lipid peroxidation in response to the generation of ROS.

GPxs have been known to contain Sec at their catalytic site, which is co-translationally inserted in response to the UGA codon, a stop signal in the standard genetic code. The alternative decoding of UGA generally depends on a *cis*-factor, called SECIS, which is located in the 3′-UTR of these selenoprotein genes (Stadtman, 1996). In our analysis, however, the selenium-dependent GPxs (sGPxs) showed a biased distributional pattern across diverse eukaryotic domains. The Sec codon and the concurrent SECIS motif were detected exclusively within the mRNA sequences of the trematode and vertebrate GPxs. Among the trematode enzymes obtainable, only PwGPx1 was determined to be a selenium-independent GPx (siGPx). The *GPx* genes retrieved from the other taxa did not contain the Sec-related sequence factors, with an exception of one isolated from an arachnidal tick. Regarding catalytic activity, the lower redox potential of selenol in Sec ($pK_a = 5{\cdot}2$) than thiol in cysteine ($pK_a \geqslant 8{\cdot}0$) is favourable for the conversion of the reduced enzyme into the oxidized form, and thus sGPx seems to be more catalytically active than siGPx, under physiological conditions (Stadtman, 1996). The siGPx has been postulated either to comprise a second-line defence or to cooperate with sGPx in an as yet unknown novel manner, to cope with cellular oxidative stresses (Utomo *et al*. 2004). It is also possible that siGPx performs a role as an antioxidant enzyme in special microenvironments, considering the effect of the surrounding pH on the ionizing potential of the normal thiol in cysteine. The siGPxs of filarial nematodes, of which functions are mainly confined at the cuticular matrix, are likely to be an example of the second suggestion (Cookson *et al*. 1992). Our results demonstrated that the induction level of Sec-independent PwGPx1 was much higher than that of Sec-dependent PwGPx2, either during development of *P. westermani* or against exogenous oxidative stresses. We are currently designing a study to observe whether the difference in the transcriptional activity is associated with the differential catalytic potentials and/or whether the two enzymes exert their effects within each of specific microniches in vitellocytes.

Among the 6 families of GPx isoenzymes, the PHGPxs have been exclusively isolated in trematodes and arthropods, whereas the GPx3 homologues have been identified as a major GPx family responsible for anti-oxidative defence in the parasitic nematodes. In contrast to the inconsistently conserved structures of the *PHGPx* genes across taxa, nematode and vertebrate genes encoding the GPx3-like proteins possessed an intron shared by all of the genes examined (unpublished data). The differentially preserved genomic structures across eukaryotic domains reflected that the *GPx* genes have multiple origins in the evolutionary episode of diverse eukaryotic domains; several paralogues, which are multiplied during early stage of eukaryotic evolution, may have evolved variably and one or a few paralogue lineages are likely to have been maintained in each of the taxonomical clades. The 2 subclade genes found in trematodes seem to have been duplicated after the divergence of Trematoda from the other animal domains. Investigations on these biased evolutionary pathways of the *GPx* genes along with the lower animal taxa, especially in association with their specialized functions, will provide us more detailed knowledge regarding the biological implications of this antioxidant enzyme system.

This work was supported by the Anti-Communicable Diseases Control Program of the National Institute of Health (NIH 348-6111-215), National Research and Development Program, Ministry of Health and Welfare, Korea and also by a research grant from the Samsung Biomedical Research Institute, #SBRI B-A2-006. Seon-Hee Kim was financially supported by the Brain Korea 21.

REFERENCES

Arthur, J. R. (2000). The glutathione peroxidases. *Cellular and Molecular Life Sciences* **57**, 1825–1835.

Blair, D., Xu, Z. B. and Agatsuma, T. (1999). Paragonimiasis and the genus *Paragonimus*. *Advances in Parasitology* **42**, 113–222.

Brigelius-Flohé, R., Aumann, K. D., Blöcker, H., Gross, G., Kiess, M., Klöppel, K. D., Maiorino, M., Roveri, A., Schuckelt, R., Ursini, F., Wingender, E. and Flohé, L. (1994). Phospholipid-hydroperoxide glutathione peroxidase. Genomic DNA, cDNA, and deduced amino acid sequence. *Journal of Biological Chemistry* **269**, 7342–7348.

Cai, G. B., Bae, Y. A., Kim, S. H., Sohn, W. M., Lee, Y. S., Jiang, M. S., Kim, T. S. and Kong, Y. (2008). Vitellocye-specific expression of hydroperoxide glutathione peroxidases in *Clonorchis sinensis*. *International Journal for Parasitology* **38**, 1613–1623.

Callahan, H. L., Crouch, R. K. and James, E. R. (1988). Helminth anti-oxidant enzymes: a protective mechanism against host oxidants? *Parasitology Today* **4**, 218–225.

Chi, C., Tanaka, R., Okuda, Y., Ikota, N., Yamamoto, H., Urano, S., Ozawa, T. and Anzai, K. (2005). Quantitative measurements of oxidative stress in mouse skin induced by X-ray irradiation. *Chemical and Pharmaceutical Bulletin* **53**, 1411–1415.

Chung, Y. B., Lee, H. S., Song, C. Y. and Cho, S. Y. (1992). Activities of scavenging enzymes of oxygen radicals in early maturation stages of *Paragonimus westermani*. *Korean Journal of Parasitology* **30**, 355–358.

Comhair, A. A. and Erzurum, S. C. (2005). The regulation and role of extracellular glutathione peroxidase. *Antioxidants & Redox Signaling* **7**, 72–79.

Cookson, E., Blaxter, M. L. and Selkirk, M. E. (1992). Identification of the major soluble cuticular glycoprotein of lymphatic filarial nematode parasites (gp29) as a secretory homolog of glutathione peroxidase, *Proceedings of the National Academy of Sciences, USA* **89**, 5837–5841.

Dröge, W. (2002). Free radicals in the physiological control of cell function. *Physiological Reviews* **82**, 47–95.

Epp, O., Ladenstein, R. and Wendel, A. (1983). The refined structure of the selenoenzyme glutathione peroxidase at 0·2-nm resolution. *European Journal of Biochemistry* **133**, 51–69.

Grossmann, A. and Wendel, A. (1983). Non-reactivity of the selenoenzyme glutathione peroxidase with enzymatically hydroperoxidized phospholipids. *European Journal of Biochemistry* **135**, 549–552.

Hancock, J. T., Desikan, R. and Neill, S. J. (2001). Role of reactive oxygen species in cell signalling pathways. *Biochemistry Society Transactions* **29**, 345–350.

Henkle-Dührsen, K. and Kampkötter, A. (2001). Antioxidant enzyme families in parasitic nematodes. *Molecular and Biochemical Parasitology* **114**, 129–142.

Hong, S. J., Kang, S. Y., Chung, Y. B., Chung, M. H., Oh, Y. J., Kang, I., Bahk, Y. Y., Kong, Y. and Cho, S. Y. (2000). *Paragonimus westermani*: a cytosolic glutathione S-transferase of a sigma-class in adult stage. *Experimental Parasitology* **94**, 180–189.

Imai, H. and Nakagawa, Y. (2003). Biological significance of phospholipids hydroperoxide glutathione peroxidase (PHGPx, GPx4) in mammalian cells. *Free Radical Biology & Medicine* **34**, 145–169.

Jackson, M. J. (2005). Reactive oxygen species and redox-regulation of skeletal muscle adaptations to exercise. *Philosophical Transactions of the Royal Society of London, B* **360**, 2285–2291.

Kryukov, G. V., Castellano, S., Novoselov, S. V., Lobanov, A. V., Zehtab, O., Guigó, R. and Gladyshev, V. N. (2003). Characterization of mammalian selenoproteomes, *Science* **300**, 1439–1443.

Li, A. H., Na, B. K., Kong, Y., Cho, S. H., Zhao, Q. P. and Kim, T. S. (2005). Molecular cloning and characterization of copper/zinc-superoxide dismutase of *Paragonimus westermani*. *Journal of Parasitology* **91**, 293–299.

Mei, H. and LoVerde, P. T. (1995). *Schistosoma mansoni*: cloning the gene encoding glutathione peroxidase. *Experimental Parasitology* **80**, 319–322.

Nakamura-Uchiyama, F., Mukae, H. and Nawa, Y. (2002). Paragonimiasis: a Japanese perspective. *Clinics in Chest Medicine* **23**, 409–420.

O'Brien, P. J. (1991). Molecular mechanisms of quinone cytotoxicity. *Chemico-biological Interactions* **80**, 1–41.

Roche, C., Liu, J. L., LePresle, T., Capron, A. and Pierce, R. J. (1996). Tissue localization and stage-specific expression of the phospholipid hydroperoxide glutathione peroxidase of *Schistosoma mansoni*. *Molecular and Biochemical Parasitology* **75**, 187–195.

Salinas, G., Selkirk, M. E., Chalar, C., Maizels, R. M. and Fernandez, C. (2004). Linked thioredoxin-glutathione systems in platyhelminths. *Trends in Parasitology* **20**, 340–346.

Sayed, A. A., Cook, S. K. and Williams, D. L. (2006). Redox balance mechanisms in *Schistosoma mansoni* rely on peroxiredoxins and albumin and implicate peroxiredoxins as novel drug targets. *Journal of Biological Chemistry* **281**, 17001–17010.

Selkirk, M. E., Smith, V. P., Thomas, G. R. and Gounaris, K. (1998). Resistance of filarial nematode parasites to oxidative stress. *International Journal for Parasitology* **28**, 1315–1332.

Sim, S., Yong, T. S., Park, S. J., Im, K. I., Kong, Y., Ryu, J. S., Min, D. Y. and Shin, M. H. (2005). NADPH oxidase-derived reactive oxygen species-mediated activation of ERK1/2 is required for apoptosis of human neutrophils induced by *Entamoeba histolytica*. *Journal of Immunology* **174**, 4279–4288.

Stadtman, T. C. (1996). Selenocysteine. *Annual Review of Biochemistry* **65**, 83–100.

Tawe, W. N., Eschbach, M. L., Walter, R. D. and Henkle-Dührsen, K. (1998). Identification of stress-responsive genes in *Caenorhabditis elegans* using RT-PCR differential display. *Nucleic acids Research* **26**, 1621–1627.

Thannickal, V. J. and Fanburg, B. L. (2000). Reactive oxygen species in cell signaling. *American Journal of Physiology. Lung Cellular and Molecular Physiology* **279**, L1005–1028.

Ursini, F. and Bindoli, A. (1987). The role of selenium peroxidases in the protection against oxidative damage of membranes. *Chemistry and Physics of Lipids* **44**, 255–276.

Utomo, A., Jiang, X., Furuta, S., Yun, J., Levin, D. S., Wang, Y. C., Desai, K. V., Green, J. E., Chen, P. L. and Lee, W. H. (2004). Identification of a novel putative non-selenocysteine containing phospholipids hydroperoxide glutathione peroxidase (NPGPx) essential for alleviating oxidative stress generated from polyunsaturated fatty acids in breast cancer cells. *Journal of Biological Chemistry* **279**, 43522–43529.

Williams, D. L., Pierce, R. J., Cookson, E. and Capron, A. (1992). Molecular cloning and sequencing of glutathione peroxidase from *Schistosoma mansoni*. *Molecular and Biochemical Parasitology* **52**, 127–130.

World Health Organization (1995). Report on control of food-borne trematode infections. *WHO Technical Report Series No. 849*. World Health Organization, Geneva.

Zelck, U. E. and von Janowsky, B. (2004). Antioxidant enzymes in intramolluscan *Schistosoma mansoni* and ROS-induced changes in expression. *Parasitology* **128**, 493–501.